CHEMISTRY OF MATERIALS
Cite This: Chem. Mater. 2019, 31, 1500−1506
Article
pubs.acs.org/cm

A Freely Soluble, High Electron Affinity Molecular Dopant for Solution Processing of Organic Semiconductors

Jan Saska,[†] Goktug Gonel,[§] Zaira I. Bedolla-Valdez,[§] Sean D. Aronow,[†] Nikolay E. Shevchenko,[†] Alexander S. Dudnik,[†] Adam J. Moulé,*[,§] and Mark Mascal*[,†]

[†]Department of Chemistry and [§]Department of Chemical Engineering, University of California, Davis, California 95616, United States

Supporting Information

ABSTRACT: Molecular dopants are increasingly studied to enhance the conductivity of semiconducting polymers. Most available p-type dopants have low solubility in common solvents and moderate electron affinities (EA), which makes solution processing difficult and limits the range of semiconducting polymers that can be doped. Here, we describe the synthesis and characterization of the new molecular dopant TMCN3-CP, which has an EA of −5.5 eV. We show that high ionization energy alternating copolymers such as PDPP-4T, PDPP-3T, and PDPP-T-TT-T can be p-type doped and achieve high conductivities with TMCN3-CP using sequential solution processing. The main advantage of this new dopant is the ability to chemically tailor the ester groups, which we demonstrate here for sequential solution doping of films. Sequential solution processing allows a greater ability to control the film morphology and is also desirable for scale-up to large-area polymer electronics.

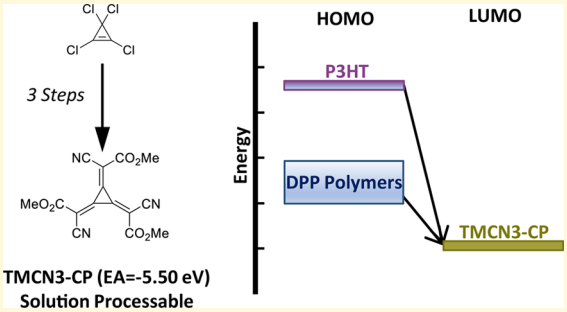

INTRODUCTION

Stimulated by the continual drive for innovation in microelectronics, the development of organic semiconductors (OSCs) as the basis for solution-processable organic field-effect transistors (OFETs) has become a major field of research, most of which focuses on the development of polymeric and molecular p-type, or hole-transporting, organic materials.[1,2] Due to their low cost, light weight, flexibility, and low environmental footprint,[3−5] OSCs are particularly useful for applications such as flexible displays,[6] chemical sensors,[5] and organic photovoltaics.[7]

Molecular p-type dopants are relatively small neutral organic species with high electron affinities that can accept electrons from OSCs, leading to an increase in the number of free charges, which results in multiple orders of magnitude increases in conductivity.[8,9] As the range of OSCs broadens both in structure and electronic properties, a new generation of dopants has been developed to improve the performance of the devices derived therefrom.

Currently, the most widely studied and used organic dopant is 2,3,5,6-tetrafluoro-7,7,8,8-tetracyanoquinodimethane (F4TCNQ).[10] Indeed, a search of the *Chemical Abstracts* database finds nearly 2000 journal articles and patents in which F4TCNQ appears in one context or another. A major challenge however has been to develop dopants that keep pace with the decreasing HOMO energy levels of higher performance materials. F4TCNQ has a measured electron affinity (EA) of −5.24 eV,[10] which is adequate in combination with relatively electron-rich polymers such as poly(3-hexylthiophene) (P3HT).[11,12] However, more advanced OSCs tend toward higher ionization energies,[2,13−15] and many cannot therefore be effectively doped with F4TCNQ. This fact has led to a growing interest in dopants with ultralow LUMO energies, and the past decade has seen reports of the synthesis of 1,3,4,5,7,8-hexafluorotetracyanonaphthoquinodimethane (F6-TCNNQ; EA = −5.37 eV),[16] 3,6-difluoro-2,5,7,7,8,8-hexacyanoquinodimethane (F2-HCNQ; EA = −5.59 eV),[17] and molybdenum tris(1,2-bis(trifluoromethyl-)ethane-1,2-dithiolene) [Mo(tfd)$_3$, EA = −5.60 eV] (Figure 1).[18] The strongest molecular dopant to date is hexacyanotrimethylenecyclopropane (CN6-CP, EA = −5.87 eV), as reported by Karpov et al.,[19] although its original synthesis dates back to the 1970s.[20−22]

Yet another hurdle is to identify dopants that enable the application of solution processing of semiconducting polymers, such as spin coating, screen printing, and inkjet printing.[23] Unfortunately, all of the above described dopants generally suffer from poor solubility in common organic solvents. As a result, they have to be introduced into OSCs either by evaporation processes[10,24] or premixing in an inert matrix.[25,26] This restricts development of technologies to mass-produce organic electronics, which depends on solution processing.[8,23] In an effort to address this problem, Marder et al. reported the synthesis of molybdenum tris-(1-(methoxycarbonyl)-2-

Received: September 29, 2018
Revised: February 4, 2019
Published: February 18, 2019

DOI: 10.1021/acs.chemmater.8b04150
Chem. Mater. 2019, 31, 1500−1506

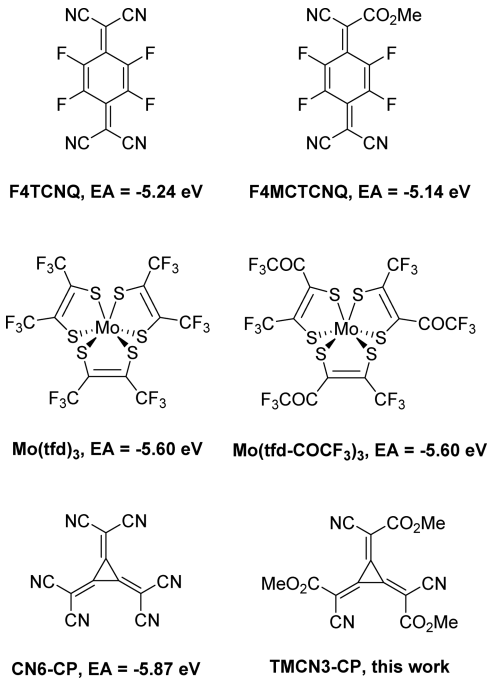

Figure 1. Structures of representative molecular dopants and their soluble analogues.

(trifluoromethyl)ethane-1,2-dithiolene) [$Mo(tfd\text{-}CO_2Me)_3$] (Figure 1),[27,28] an analogue of $Mo(tfd)_3$ with solubility nearly 20 times higher, albeit at the cost of a dramatically reduced EA (5.00 eV). The same group has also reported molybdenum tris(1-(trifluoromethylcarbonyl)-2-(trifluoromethyl)-ethane1,2-dithiolene) [$Mo(tfd\text{-}COCF_3)_3$], which has a solubility comparable to $Mo(tfd\text{-}CO_2Me)_3$ and yet an EA equivalent to $Mo(tfd)_3$.[29,30] In our own approach,[31] we prepared a series of F4TCNQ analogues wherein one or two of the nitrile functional groups were replaced with either methyl or octyl esters. It has been shown that these ester analogues exhibit an increase in solubility by a factor of up to 100, while the EAs were only reduced by approximately 0.1 eV per ester group substituent. At the same time, it was observed that increased solubility leads to an increase in doping efficiency, such that higher conductivities in P3HT were achieved with F4MCTCNQ than F4TCNQ, despite the lower EA of the former.

Along with EA and solubility, a third issue in dopant design for organic electronic devices is control of the dopant diffusion and drift.[8,32] In order for devices to be durable, dopants must remain in the domain in which they were printed and not diffuse or drift from their initial position. Volatile dopants like I_2 for example are particularly difficult to process because they sublime out of the polymer at room temperature.[33] We recently demonstrated that dopant diffusion, which has negative effects both on device performance and lifetime,[34,35] is significantly reduced by the substitution of even one nitrile group in F4TCNQ for a methyl ester.[34]

Applying the same molecular design principles, we now present a simple and efficient synthesis of the high EA soluble molecular dopant trimethyl 2,2′,2″-(cyclopropane-1,2,3-triylidene)-tris(cyanoacetate) (TMCN3-CP), an analogue of CN6-CP in which three of the six nitrile groups are replaced with methyl esters. Its electrochemical properties measured using cyclic voltammetry (CV) are reported. Additionally, a series of polymer films were sequentially doped from solution to determine the changes that TMCN3-CP induced on the optical absorbance and conductivity of the films.

P3HT has a reported ionization energy of 4.4−5.1 eV, depending on the literature source.[11,36,37] We also include in this study a series of alternating copolymers with diketopyrrolopyrrole (DPP) groups that have higher ionization energies than P3HT and cannot be effectively p-doped by F4TCNQ.[19] Supporting Information Figure S1 gives the molecular structures of these polymers, and Supporting Information Figures S2−S4 show that the addition of F4TCNQ to DPP polymers does not change the absorbance spectrum, which is a clear demonstration that no polaron states are formed. The repeating units present a common DPP acceptor moiety with a donor unit consisting of three thiophenes (3T), four thiophenes (4T), or a thiophene-thienothiophene-thiophene (T-TT-T).[38,39] These three polymers were chosen because they have been well studied for OFET applications and have high reported hole mobilities.[39,40] In addition, PDPP-4T and PDPP-T-TT-T have been recently used to study the effectiveness of p-type dopants, including $FeCl_3$, $Mo(tfd)_3$, and $Mo(tfd\text{-}CO_2Me)_3$.[41] PDPP-T-TT-T was also used to study doping by F4TCNQ, F6TCNNQ, and CN6-CP.[19,36] We show here that all three copolymers are effectively doped by sequential solution processing using TMCN3-CP. This is, to our knowledge, the first report of sequential solution doping of these high ionization energy polymers. In previous studies, the dopant was mixed into a batch solution for simultaneous deposition.[19,36,41]

EXPERIMENTAL SECTION

Materials. $CN6\text{-}CP^{\bullet-}$ was prepared according to the method published by Karpov et al.[19] Nitrosonium tertrafluoroborate and tetrachlorocyclopropene were purchased from Acros Organics. All other reagents and solvents were purchased from Sigma-Aldrich and used as supplied. PDPP-T-TT-T and PDPP-4T were purchased from Ossila. PDPP-3T was provided by the Dudnik group. P3HT was purchased from Sigma Aldrich (MW: 50000−70000, regioregularity ≥ 90%). F4TCNQ was purchased from Tokyo Chemical Industry Co., Ltd.

Characterization. ^1H and ^{13}C NMR spectra were measured using a 400 MHz Bruker Nanobay AVIIIHD spectrometer in $CDCl_3$ solvent. All chemical shifts (δ) are reported in parts per million (ppm) relative to chloroform residual solvent peaks (δ_H = 7.26 ppm, δ_C = 77.0 ppm).

Cyclic voltammograms (CVs) were recorded on a BASi Epsilon MF-9092 electrochemical workstation. Redox potentials were measured in degassed anhydrous acetonitrile solution containing tetramethylammonium tetrafluoroborate as a supporting electrolyte (0.05 M) using a platinum disk working electrode (⌀ = 1.6 mm), a glassy carbon counter electrode, and a Ag/AgCl reference electrode. The concentration of substrates in the working solution was 0.50 mM, and the electrochemical potential sweep rate was fixed at 100 mV/s.

High-resolution mass spectra (HRMS) were recorded on a Thermo Fisher Hybrid LTQ-Orbitrap XL mass spectrometer.

UV−vis−NIR spectra were measured using a PerkinElmer Lambda 750 spectrometer. The glass substrates were sequentially cleaned in ultrasonic baths of acetone, methanol, isopropanol, and deionized water, followed by drying with nitrogen. The substrates were then exposed to UV/ozone for 30 min before use. Film samples were prepared by dissolving the polymers in chlorobenzene (CB) (for P3HT) or 1:1 $CHCl_3$/CB for DPP copolymers at a concentration of 3 mg/mL. The samples were spin coated for film thicknesses of ∼50 nm. TMCN3-CP was dissolved in CH_2Cl_2 or 2:1 CH_2Cl_2/acetonitrile and sequentially coated onto the same substrate before spinning the sample to remove excess solution. Film thicknesses were measured

DOI: 10.1021/acs.chemmater.8b04150
Chem. Mater. 2019, 31, 1500−1506

with a Veeco Dektak 150 surface profilometer. All UV−vis−NIR spectra were measured under ambient conditions in air except for the time-dependent UV−vis−NIR experiments shown in Figures S9 and S12. The two samples in these figures were sealed in a nitrogen-filled glovebox (O_2 level < 10 ppm, H_2O level < 5 ppm) in a sample holder that was designed by our group.[42]

Conductivity measurements of doped films were performed with a four-point probe setup on Si substrates using a Keithley 2450 source measurement unit. Four electrodes (5 nm Cr/95 nm Au, 1 × 5 mm^2, 1 mm spacing) were deposited through a shadow mask by thermal evaporation. Neat films were measured using a two-wire probe with 10−20 μm channel length and 1−2 mm channel width. The same procedure was used for substrate cleaning and sequential film deposition as described above. All conductivity measurements were performed in the dark under a nitrogen atmosphere in a glovebox.

Synthesis of TMCN3-CP. *Potassium Trimethyl 2,2′,2″-(Cyclopropane-1,2,3-triylidene)-tris(cyanoacetate) Radical Anion (**2**).* To a suspension of sodium hydride (850 mg of a 60% dispersion in mineral oil, 21.2 mmol) in anhydrous 1,2-dimethoxyethane (9.0 mL) at 0 °C was added methyl cyanoacetate (0.740 mL, 829 mg, 8.42 mmol) and the reaction mixture was stirred at rt for 1 h. Tetrachlorocyclopropene **1** (0.360 mL, 522 mg, 2.95 mmol) was added dropwise, and the mixture was stirred for a further 2 h during which an orange precipitate formed. The precipitate was collected by vacuum filtration, washed with Et_2O, and introduced in a single portion into a solution of potassium persulfate (1.14 g, 4.20 mmol) in water (50 mL). The resulting deep purple mixture was stirred at rt for 3 h during which a purple precipitate formed. This precipitate was collected by vacuum filtration, washed with water (×3), and dried under high vacuum for 16 h to give **2** (727 mg, 71%) as a purple powder.

HRMS (ESI$^-$) $C_{15}H_9N_3O_6^-$ $[M]^-$ m/z calcd. 327.0491, found 327.0500; mp 242 °C (dec).

NMR spectra of **2** could not be obtained due to the open shell nature of the compound.

Trimethyl 2,2′,2″-(Cyclopropane-1,2,3-triylidene)-tris-(cyanoacetate) (TMCN3-CP). All operations were performed in a glovebox under a dry nitrogen atmosphere. To a suspension of **2** (100 mg, 0.27 mmol) in anhydrous CH_2Cl_2 (1.0 mL) was added $NOBF_4$ (157 mg, 1.35 mmol), and the mixture was stirred for 30 min. The solids were removed by filtration and the filtrate was diluted with hexane (50 mL). The resulting yellow precipitate was collected by filtration and dried in a stream of nitrogen for 3 h to give TMCN3-CP (64.0 mg, 72%).

^{1}H NMR (400 MHz, $CDCl_3$) δ 4.08 (s, 3H); ^{13}C NMR (101 MHz, $CDCl_3$) δ 160.0, 128.6, 113.7, 103.8, 56.1; HRMS (ESI$^-$) $C_{15}H_9N_3O_6^-$ $[M]^-$ m/z calcd. 327.0491, found 327.0500; mp 108 °C (dec).

RESULTS AND DISCUSSION

Synthesis of TMCN3-CP. TMCN3-CP was prepared using a modification of Karpov et al's protocol for synthesis of CN6-CP (Scheme 1).[19] To this end, tetrachlorocylopropene **1** was treated with methyl cyanoacetate in the presence of excess sodium hydride to give the bis-sodium salt of TMCN3-CP^{2-}, which was immediately subjected to oxidation with an aqueous solution of potassium persulfate to give the radical anion salt **2** in good yield. While the radical anion salt of TMCN3-CP **2** is a known compound,[22] to the best of our knowledge, no synthesis of the fully oxidized neutral molecule has been reported to date. We have found this salt to be remarkably stable and were able to prepare and store multigram quantities of the material in air without it showing any signs of deterioration. Next, a second one-electron oxidation was performed using nitrosonium tetrafluoroborate. Any excess of this poorly soluble oxidant could be simply removed from the reaction mixture by filtration, and upon addition of hexane, pure TMCN3-CP precipitated out of solution as a yellow

Scheme 1. Synthesis of TMCN3-CP[a]

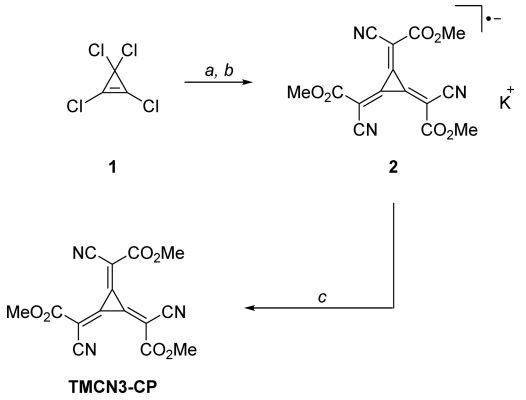

[a]Reagents and conditions: *a*. methyl cyanoacetate, NaH, DME, 3 h; *b*. $K_2S_2O_8$, H_2O, 3 h, 71% over 2 steps; *c*. $NOBF_4$, CH_2Cl_2, 30 min, 72%.

powder. The assigned C_3 symmetric structure of TMCN3-CP was confirmed by NMR. It is important to note that, unlike its precursor **2**, TMCN3-CP is highly air- and moisture-sensitive, and all stages of the final synthetic step should be carried out in a glovebox using anhydrous solvents. Longer term storage of TMCN3-CP is best achieved under vacuum.

Dopant Characterization. With sufficient quantities (>200 mg) of TMCN3-CP in hand, we set out to identify solvents in which it could be handled without decomposition. As expected, TMCN3-CP reacted almost immediately with all polar protic (ROH) and most aprotic solvents (acetone, DMSO, aromatics) to which it was subjected. Even dry MeCN only had a 1−2 min window before some degree of discoloration could be seen. We did, however, find TMCN3-CP to be both readily soluble and stable over a period of several hours in halogenated solvents including chloroform, dichloromethane, and hexafluorobenzene. As a result, we were able to perform full characterization and structural assignment of the molecule using conventional NMR techniques.

To estimate the reduction potentials and, by extension, the EA of this new dopant molecule, we conducted a series of CV measurements (Figure 2). Predictably, we observe two reversible one-electron reductions corresponding to formation of TMCN3-CP$^{\bullet-}$ and TMCN3-CP^{2-}. These occur at E_{red1} = 0.78 V and E_{red2} = 0.12 V versus Ag/AgCl, respectively. According to the equation $E_{LUMO} = -e(E_{red} + E_{ref})$, where E_{ref}

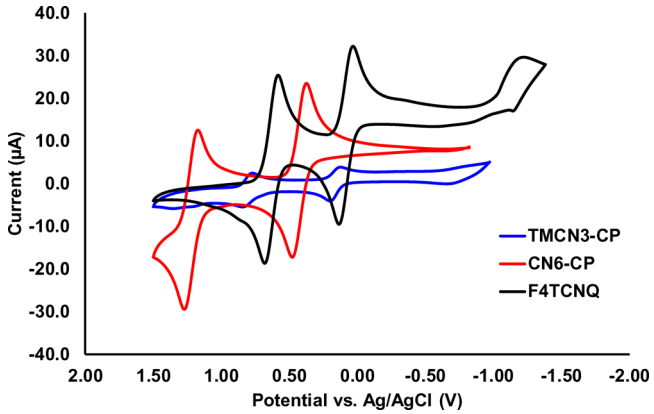

Figure 2. Cyclic voltammograms of TMCN3-CP, CN6-CP, and F4TCNQ.

DOI: 10.1021/acs.chemmater.8b04150
Chem. Mater. 2019, 31, 1500−1506

= 4.72 V for the Ag/AgCl reference electrode used in our measurements,[17] we calculate the LUMO levels for TMCN3-CP to be E_{LUMO1} = −5.50 eV and E_{LUMO2} = −4.84 eV.

The accuracy of these values was substantiated by conducting the same measurements on commercial F4TCNQ and CN6-CP$^{\bullet-}$, which was prepared according to the literature method.[19] The LUMO levels for both F4TCNQ (E_{LUMO1} = −5.30 eV) and CN6-CP (E_{LUMO1} = −5.89 eV) were in excellent agreement with previously published values (E_{LUMO1} = −5.33 eV[17] and E_{LUMO1} = −5.87 eV,[19] respectively) based on CV measurements. All measured reduction potentials and calculated LUMO energy levels are summarized in Table 1.

Table 1. Measured Reduction Potentials and Calculated LUMO Levels of TMCN3-CP, CN6-CP, and F4TCNQ

dopant	E_{red1} (V)	E_{LUMO1} (eV)	E_{red2} (V)	E_{LUMO2} (eV)
CN6-CP	1.17	−5.89	0.38	−5.10
TMCN3-CP	0.78	−5.50	0.12	−4.84
F4TCNQ	0.58	−5.30	0.03	−4.75

Figure 3 shows the UV−vis−NIR spectra of P3HT, PDPP-4T, PDPP-T-TT-T, and PDPP-3T that are doped by increasingly higher concentration solutions of TMCN3-CP. Sequential doping requires that the dopant solution be applied from a solvent that will not dissolve the polymer film. For the P3HT samples, all sequential doping was carried out in CH_2Cl_2 solution. For the DPP polymers, a 1:1 mixture of dry CH_2Cl_2/MeCN was used to prevent dissolution of the polymer films.

Examination of the UV−vis−NIR spectra shows a decrease in the absorbance of the neutral polymer and a simultaneous absorbance increase below the neat polymer optical band gap. The absorbance for P3HT has previously been assigned as P3HT$^+$ polaron absorbance in the range of 1−2 eV and centered at ∼0.5 eV.[43,44] For P3HT, almost all measurements have shown integer charge transfer with the exception of one report of a thermally unstable polymorph of P3HT with F4TCNQ.[45] Most alternating copolymers with strong acceptor groups exhibit only partial charge transfer when molecularly doped.[44] It was not the purpose of this work to assign a doping mechanism for the DPP polymers. We note instead that, with increasing TMCN3-CP concentration, the DPP copolymers all show increasing absorbance at ∼0.88 eV and below the low energy side of the spectrum (<0.4 eV), consistent with previously reported p-doping by CN6-CP.[19] We also note that previous reports of the doping of PDPP-T-TT-T by F6TCNNQ did not have a similar absorption change and partial charge transfer was determined.[36]

Sequential doping is described by an equilibrium between dopants in the solution and film.[26] The driving force for charge transfer from the polymer to the dopant is ΔG for the reaction $\text{dopant}_{solution} + \text{polymer}_{film} \rightleftharpoons \text{dopant}_{film}^{\bullet-} + \text{polymer}_{film}^{\bullet+}$ and can be approximated by $\text{HOMO}_{polymer} - \text{LUMO}_{dopant}$. Dopants occupy sites on the polymer according to a Langmuir isotherm model given by

$$C_{d,sat} - C_d = \frac{K_{eq}C_s}{1 + K_{eq}C_s} \quad (1)$$

where C_d is the polaron concentration in the film, $C_{d,sat}$ is the total concentration of sites that could be doped from a solution at infinite concentration, C_s is the concentration of the dopant in solution, and K_{eq} is the equilibrium constant determined from ΔG.[26]

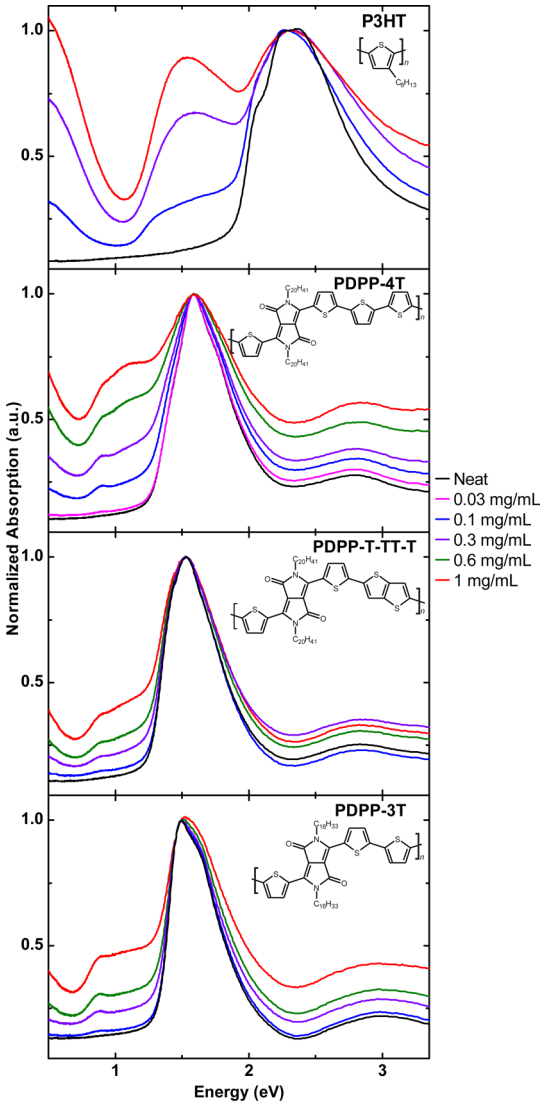

Figure 3. UV−vis−NIR spectra of P3HT, PDPP-4T, PDPP-T-TT-T, and PDPP-3T sequentially doped by solutions of TMCN3-CP. All measurements are normalized to the neat polymer absorbance maximum.

It has often been reported that the efficiency of free charge creation from molecular doping is much less than unity.[9,43,46] UV−vis−NIR cannot measure the creation of free charges but does give a measure of C_d in the polymer. In Supporting Information Figure S5, we show the change in the ratio of absorbance at the peak of the polaron state (1.52 eV for P3HT and 0.88 for all DPP polymers) compared to the absorbance maximum of the neutral polymer. Thus, we measure $(A_{doped} - A_{neutral})_{polaron\_max}/(A_{neutral})_{neutral\_max}$ as a function of the doping solution concentration. The data show a high slope at low dopant concentrations of P3HT and PDPP-4T followed by a reduction in the slope with higher dopant concentrations. This follows the expected trend that polarons are created efficiently at low doping levels and as the Fermi level shifts towards the polymer HOMO, doping efficiency is reduced.[46] In contrast, both PDPP-T-TT-T and PDPP-3T show a low and linear increase in polaron density with increased dopant concen-

DOI: 10.1021/acs.chemmater.8b04150
Chem. Mater. 2019, 31, 1500−1506

tration, which indicates that these polymers are more difficult to dope. The IE of the DPP polymers has been measured using ultraviolet photoelectron spectroscopy by several groups to be in the same range, that is, 5.17−5.40 eV, but the relative IE between polymers is not consistent.[38−40] Given the dispersity of the measured IE values, we cannot assign the IE of these polymers directly or the ΔG for doping. Our results instead show that C_d is higher for this PDPP-4T sample than the other DPP polymers. This increased doping level could originate from either a lower IE or larger $C_{d,sat}$ afforded by increased solvent swelling. This work shows that the doping efficiency depends not just on the driving force for doping (ΔG) but also on the volume density of doping sites $C_{s,sat}$ and access to these sites via solvent infiltration into the swollen polymer. The effects of molecular weight, polymer orientation, and side chain length or branching are matters for separate study.

Figure 4 shows the four-wire conductivity (σ) for all polymer films plotted as a function of the concentration of

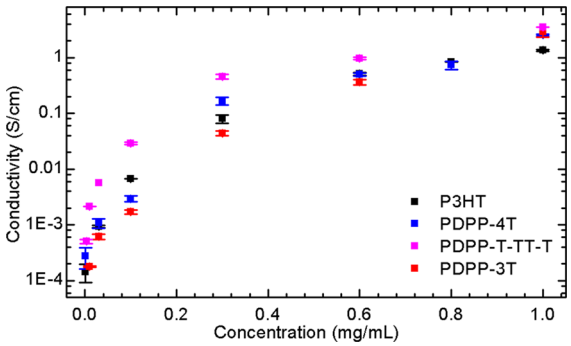

Figure 4. Four-wire conductivity measurements for P3HT, PDPP-4T, PDPP-T-TT-T, and PDPP-3T as a function of the TMCN3-CP sequential doping concentration.

TMCN3-CP used for sequential doping. The σ of all four films increases to above 1 S/cm^2 when sequentially doped from a solution of 1 mg/mL TMCN3-CP. The PDPP-T-TT-T film has the highest σ for all doping concentrations in spite of the fact that there are fewer polaron states than for P3HT or PDPP-4T. σ is a product of the density of mobile holes and the hole mobility (μ_h). PDPP-T-TT-T has the highest reported optimized μ_h of the three polymers at 5−10 cm^2/(V·s).[47] The reported μ_h values for PDPP-4T, PDPP-3T, and P3HT are 0.5−1.5,[48] 0.5−2,[38,40,49] and 0.1−0.3 cm^2/(V·s),[50] respectively. All reported μ_h values were measured with field-effect transistors. Although C_d is lower in PDPP-T-TT-T, some combination of the high μ_h and/or a larger percentage of the polarons being free holes gives the highest σ for all doping concentrations. P3HT has much higher C_d but lower μ_h and/or free hole density and so has a similar σ value to the other polymers.

Comparing these results to other recent doping studies of DPP polymers, Liang et al. recently reported mixed batch σ measurements of PDPP-4T and PDPP-T-TT-T doped with $FeCl_3$ and $Mo(tfd)_3$.[41] At all doping ratios, PDPP-4T showed higher conductivity for both dopants, which they attributed to a higher IE for PDPP-T-TT-T. The conductivity shown here is similar for PDPP-4T but higher for PDPP-T-TT-T. The comparison with this data does not mean that TMCN3-CP is a higher EA dopant than $Mo(tfd)_3$, because the samples were prepared differently (batch vs sequential doping). The result does however clearly show that TMCN3-CP is more effective at doping PDPP-T-TT-T than $Mo(tfd)_3$ using solution methods, while both dopants have a similar ability to dope P3HT and PDPP-4T. Karpov et al. recently reported the doping of PDPP-T-TT-T and P3HT samples with F6TCNNQ[36] and CN6-CP.[19] For PDPP-T-TT-T, doping with F6TCNNQ resulted in a σ of ∼1 S/cm with a fairly low doping ratio but no increase with increased F6TCNNQ concentration. The conductivity of P3HT was higher when doped with F6TCNNQ.[36] Doping PDPP-T-TT-T with CN6-CP resulted in σ of almost 100 S/cm at a high doping ratio, which shows that higher EA dopants can yield greater increases in conductivity. To our knowledge, there are no other reports of molecular doping of PDPP-3T.

Lastly, we investigated the stability of doped polymer films. We performed sequential σ measurements over 7 days on TMCN3-CP- and F4TCNQ-doped P3HT films stored in four different environments. The samples were either kept under vacuum, in a glovebox filled with nitrogen (O_2 < 10 ppm and H_2O < 5 ppm), on a hot plate (60 °C) in the glovebox, and in air. Independent of the environment in which the samples were stored, the σ of all films decreased exponentially as shown in Figure S6, though the rate of σ decrease was lowest for the samples in the glovebox. We observed similar trends for conductivity of P3HT/F4TCNQ films as P3HT/TMCN3-CP films (Figure S7). It is important to note that organic molecular dopants have been shown to diffuse and drift in a polymer film.[8,32,34] Since we made repeated conductivity measurements on the same films, it is likely that the dopants drift away from the anode, which in turn decreases the conductivity.[32] This indicates that the evaluation of the chemical stability of the dopants is not a simple matter of monitoring the conductivity.

An alternative probe of doping density over time is to monitor the UV−vis−NIR spectra, which can resolve whether the decrease in conductivity is due to dopant drift or chemical degradation of the dopant. We thus measured the UV−vis−NIR spectra for P3HT/TMCN3-CP and P3HT/F4TCNQ films stored in air and nitrogen continuously for 20 h. In Figures S8−S13, we track the changes in the peak of neutral P3HT absorbance (∼2.2 eV) and the $P3HT^+$ polaron peak (1−2 eV). P3HT/TMCN3-CP films show a steady reduction in polaron density with time, with similar time constants for samples both in air and in a glovebox. This result suggests that the instability of the dopant in the film is not due to the reaction with O_2 or H_2O. We suspect, but cannot prove, a dimerization of the dopant radical anion similar to that observed for diester-substituted F4TCNQ.[51] In contrast, P3HT/F4TCNQ films in nitrogen show no optical change, but films in air show a slow reduction in polaron states and an increase in neutral P3HT absorbance. F4TCNQ reacts with atmospheric O_2 and/or H_2O but shows long-time stability in N_2.

Since conductivity measurements cannot alone be used to determine dopant stability due to drift, the challenge will be to synthesize high EA dopants that are chemically stable, resistant to drift, and solution processable.

CONCLUSIONS

In conclusion, we describe the synthesis of TMCN3-CP, a new, solution processable, and thermally stable p-type dopant possessing three ester groups that allow the molecule to be chemically tailored. The high solubility and EA of TMCN3-CP enable sequential molecular doping of a series of high IE

DOI: 10.1021/acs.chemmater.8b04150
Chem. Mater. 2019, 31, 1500−1506

conjugated polymers used in organic field-effect transistors. TMCN3-CP was added to the polymer films in a sequential solution processing step, resulting in clear p-type doping of P3HT, PDPP-4T, PDPP-T-TT-T, and PDPP-3T, whereas no polaron states were observed using F4TCNQ for the DPP-derived copolymers. At 1 mg/mL dopant concentration, all four polymers achieve conductivities of >1 S/cm. With lower dopant concentrations, the conductivity varied over a wider range, showing the need for in-depth studies of the effects of ionization energy and morphology on doping efficiency and the ratio between polarons and free holes. PDPP-T-TT-T polymer films exhibit lower conductivity when doped with TMCN3-CP than with CN6-CP but higher than with $Mo(tfd)_3$, $FeCl_3$, or F6TCNNQ. This study demonstrates the value of developing strong dopants with high solubilities. Further extension of this work will consider mono- and diester substitutions of CN6-CP, which should retain solubility but have even higher EA values than TMCN3-CP, and work along these lines will be reported in due course.

■ ASSOCIATED CONTENT

Supporting Information

The Supporting Information is available free of charge on the ACS Publications website at DOI: 10.1021/acs.chemmater.8b04150.

Molecular structures of all polymers used in this work; UV−vis−NIR curves of neat PDPP-4T, PDPP-T-TT-T, and PDPP-3T plotted with curves of the same polymer doped with F4TCNQ; plot of the ratio between the differential absorbance at the polaron maximum to the absorbance at the neutral polymer absorbance maximum for P3HT, PDPP-4T, PDPP-T-TT-T, and PDPP-3T doped with TMCN3-CP; ^{1}H-NMR spectrum of TMCN3-CP; ^{13}C-NMR spectrum of TMCN3-CP (PDF)

■ AUTHOR INFORMATION

Corresponding Authors

*E-mail: amoule@ucdavis.edu (A.J.M.).
*E-mail: mjmascal@ucdavis.edu (M.M.).

ORCID

Alexander S. Dudnik: 0000-0001-9014-7660
Adam J. Moulé: 0000-0003-1354-3517
Mark Mascal: 0000-0001-7841-253X

Notes

The authors declare no competing financial interest.

■ ACKNOWLEDGMENTS

This research was supported by the National Science Foundation grant 1636385. Z.I.B.-V. acknowledges the support of SENER CONACyT project 291145.

■ REFERENCES

(1) Forrest, S. R. The Path to Ubiquitous and Low-Cost Organic Electronic Appliances on Plastic. *Nature* **2004**, *428*, 911−918.
(2) Sirringhaus, H. 25th Anniversary Article: Organic Field-Effect Transistors: The Path Beyond Amorphous Silicon. *Adv. Mater.* **2014**, *26*, 1319−1335.
(3) Günes, S.; Neugebauer, H.; Sariciftci, N. S. Conjugated Polymer-Based Organic Solar Cells. *Chem. Rev.* **2007**, *107*, 1324−1338.
(4) Cheng, Y.-J.; Yang, S.-H.; Hsu, C.-S. Synthesis of Conjugated Polymers for Organic Solar Cell Applications. *Chem. Rev.* **2009**, *109*, 5868−5923.
(5) Rim, Y. S.; Bae, S. H.; Chen, H.; De Marco, N.; Yang, Y. Recent Progress in Materials and Devices toward Printable and Flexible Sensors. *Adv. Mater.* **2016**, *28*, 4415−4440.
(6) Gelinck, G. H.; Huitema, H. E. A.; van Veenendaal, E.; Cantatore, E.; Schrijnemakers, L.; van der Putten, J. B. P. H.; Geuns, T. C. T.; Beenhakkers, M.; Giesbers, J. B.; Huisman, B.-H.; Meijer, E. J.; Benito, E. M.; Touwslager, F. J.; Marsman, A. W.; van Rens, B. J. E.; de Leeuw, D. M. Flexible Active-Matrix Displays and Shift Registers Based on Solution-Processed Organic Transistors. *Nat. Mater.* **2004**, *3*, 106−110.
(7) Mazzio, K. A.; Luscombe, C. K. The Future of Organic Photovoltaics. *Chem. Soc. Rev.* **2015**, *44*, 78−90.
(8) Jacobs, I. E.; Moulé, A. J. Controlling Molecular Doping in Organic Semiconductors. *Adv. Mater.* **2017**, *29*, 1703063.
(9) Lüssem, B.; Keum, C.-M.; Kasemann, D.; Naab, B.; Bao, Z.; Leo, K. Doped Organic Transistors. *Chem. Rev.* **2016**, *116*, 13714−13751.
(10) Walzer, K.; Maennig, B.; Pfeiffer, M.; Leo, K. Highly Efficient Organic Devices Based on Electrically Doped Transport Layers. *Chem. Rev.* **2007**, *107*, 1233−1271.
(11) Pingel, P.; Neher, D. Comprehensive Picture of *p*-Type Doping of P3HT with the Molecular Acceptor F_4TCNQ. *Phys. Rev. B* **2013**, *87*, 115209.
(12) Pingel, P.; Schwarzl, R.; Neher, D. Effect of Molecular P-Doping on Hole Density and Mobility in Poly(3-Hexylthiophene). *Appl. Phys. Lett.* **2012**, *100*, 143303.
(13) Chen, J.; Cao, Y. Development of Novel Conjugated Donor Polymers for High-Efficiency Bulk-Heterojunction Photovoltaic Devices. *Acc. Chem. Res.* **2009**, *42*, 1709−1718.
(14) Wang, C.; Dong, H.; Hu, W.; Liu, Y.; Zhu, D. Semiconducting Π-Conjugated Systems in Field-Effect Transistors: A Material Odyssey of Organic Electronics. *Chem. Rev.* **2012**, *112*, 2208−2267.
(15) Zaumseil, J.; Sirringhaus, H. Electron and Ambipolar Transport in Organic Field-Effect Transistors. *Chem. Rev.* **2007**, *107*, 1296−1323.
(16) Koech, P. K.; Padmaperuma, A. B.; Wang, L.; Swensen, J. S.; Polikarpov, E.; Darsell, J. T.; Rainbolt, J. E.; Gaspar, D. J. Synthesis and Application of 1,3,4,5,7,8-Hexafluorotetracyanonaphthoquinodimethane (F6-TNAP): A Conductivity Dopant for Organic Light-Emitting Devices. *Chem. Mater.* **2010**, *22*, 3926−3932.
(17) Gao, Z. Q.; Mi, B. X.; Xu, G. Z.; Wan, Y. Q.; Gong, M. L.; Cheah, K. W.; Chen, C. H. An Organic P-Type Dopant with High Thermal Stability for an Organic Semiconductor. *Chem. Commun.* **2008**, 117−119.
(18) Qi, Y.; Sajoto, T.; Barlow, S.; Kim, E.-G.; Brédas, J.-L.; Marder, S. R.; Kahn, A. Use of a High Electron-Affinity Molybdenum Dithiolene Complex to P-Dope Hole-Transport Layers. *J. Am. Chem. Soc.* **2009**, *131*, 12530−12531.
(19) Karpov, Y.; Erdmann, T.; Raguzin, I.; Al-Hussein, M.; Binner, M.; Lappan, U.; Stamm, M.; Gerasimov, K. L.; Beryozkina, T.; Bakulev, V.; Anokhin, D. V.; Ivanov, D. A.; Günther, F.; Gemming, S.; Seifert, G.; Voit, B.; Di Pietro, R.; Kiriy, A. High Conductivity in Molecularly P-Doped Diketopyrrolopyrrole-Based Polymer: The Impact of a High Dopant Strength and Good Structural Order. *Adv. Mater.* **2016**, *28*, 6003−6010.
(20) Fukunaga, T. Negatively Substituted Trimethylenecyclopropane Dianions. *J. Am. Chem. Soc.* **1976**, *98*, 610−611.
(21) Fukunaga, T.; Gordon, M. D.; Krusic, P. J. Negatively Substituted Trimethylenecyclopropanes and Their Radical Anions. *J. Am. Chem. Soc.* **1976**, *98*, 611−613.
(22) Fukunaga, T. Substituted Trimethylene Cyclopropanes, Salts, and Intermediates. U.S. Patent 4,003,943A, Jan 18, 1977.
(23) Arias, A. C.; MacKenzie, J. D.; McCulloch, I.; Rivnay, J.; Salleo, A. Materials and Applications for Large Area Electronics: Solution-Based Approaches. *Chem. Rev.* **2010**, *110*, 3−24.
(24) Scholes, D. T.; Hawks, S. A.; Yee, P. Y.; Wu, H.; Lindemuth, J. R.; Tolbert, S. H.; Schwartz, B. J. Overcoming Film Quality Issues for

DOI: 10.1021/acs.chemmater.8b04150
Chem. Mater. 2019, 31, 1500−1506

Conjugated Polymers Doped with F4TCNQ by Solution Sequential Processing: Hall Effect, Structural, and Optical Measurements. *J. Phys. Chem. Lett.* **2015**, *6*, 4786−4793.
(25) Rainbolt, J. E.; Koech, P. K.; Polikarpov, E.; Swensen, J. S.; Cosimbescu, L.; Von Ruden, A.; Wang, L.; Sapochak, L. S.; Padmaperuma, A. B.; Gaspar, D. J. Synthesis and Characterization of P-Type Conductivity Dopant 2-(3-(Adamantan-1-yl)Propyl)-3,5,6-Trifluoro-7,7,8,8-Tetracyanoquinodimethane. *J. Mater. Chem. C* **2013**, *1*, 1876−1884.
(26) Jacobs, I. E.; Aasen, E. W.; Oliveira, J. L.; Fonseca, T. N.; Roehling, J. D.; Li, J.; Zhang, G.; Augustine, M. P.; Mascal, M.; Moulé, A. J. Comparison of Solution-Mixed and Sequentially Processed P3HT:F4TCNQ Films: Effect of Doping-Induced Aggregation on Film Morphology. *J. Mater. Chem. C* **2016**, *4*, 3454−3466.
(27) Dai, A.; Wan, A.; Magee, C.; Zhang, Y.; Barlow, S.; Marder, S. R.; Kahn, A. Investigation of P-Dopant Diffusion in Polymer Films and Bulk Heterojunctions: Stable Spatially-Confined Doping for All-Solution Processed Solar Cells. *Org. Electron.* **2015**, *23*, 151−157.
(28) Dai, A.; Zhou, Y.; Shu, A. L.; Mohapatra, S. K.; Wang, H.; Fuentes-Hernandez, C.; Zhang, Y.; Barlow, S.; Loo, Y.-L.; Marder, S. R.; Kippelen, B.; Kahn, A. Enhanced Charge-Carrier Injection and Collection Via Lamination of Doped Polymer Layers P-Doped with a Solution-Processible Molybdenum Complex. *Adv. Funct. Mater.* **2014**, *24*, 2197−2204.
(29) Paniagua, S. A.; Baltazar, J.; Sojoudi, H.; Mohapatra, S. K.; Zhang, S.; Henderson, C. L.; Graham, S.; Barlow, S.; Marder, S. R. Production of Heavily N-and P-Doped Cvd Graphene with Solution-Processed Redox-Active Metal−Organic Species. *Mater. Horiz.* **2014**, *1*, 111−115.
(30) Mohapatra, S. K.; Zhang, Y.; Sandhu, B.; Fonari, M. S.; Timofeeva, T. V.; Marder, S. R.; Barlow, S. Synthesis, Characterization, and Crystal Structures of Molybdenum Complexes of Unsymmetrical Electron-Poor Dithiolene Ligands. *Polyhedron* **2016**, *116*, 88−95.
(31) Li, J.; Zhang, G.; Holm, D. M.; Jacobs, I. E.; Yin, B.; Stroeve, P.; Mascal, M.; Moulé, A. J. Introducing Solubility Control for Improved Organic P-Type Dopants. *Chem. Mater.* **2015**, *27*, 5765−5774.
(32) Müller, L.; Rhim, S.-Y.; Sivanesan, V.; Wang, D.; Hietzschold, S.; Reiser, P.; Mankel, E.; Beck, S.; Barlow, S.; Marder, S. R.; Pucci, A.; Kowalsky, W.; Lovrincic, R. Electric-Field-Controlled Dopant Distribution in Organic Semiconductors. *Adv. Mater.* **2017**, *29*, 1701466.
(33) Heeger, Alan J., Sariciftci, N. S., Namdas, E. B. *Semiconducting and Metallic Polymers*; Oxford University Press: Oxford, U.K., 2010.
(34) Li, J.; Koshnick, C.; Diallo, S. O.; Ackling, S.; Huang, D. M.; Jacobs, I. E.; Harrelson, T. F.; Hong, K.; Zhang, G.; Beckett, J.; Mascal, M.; Moulé, A. J. Quantitative Measurements of the Temperature-Dependent Microscopic and Macroscopic Dynamics of a Molecular Dopant in a Conjugated Polymer. *Macromolecules* **2017**, *50*, 5476−5489.
(35) Zaikov, G. E.; Iordanskii, A. P.; Markin, V. S. *Diffusion of Electrolytes in Polymers*; CRC Press: Utrecht, Netherlands, 1988.
(36) Karpov, Y.; Erdmann, T.; Stamm, M.; Lappan, U.; Guskova, O.; Malanin, M.; Raguzin, I.; Beryozkina, T.; Bakulev, V.; Günther, F.; Gemming, S.; Seifert, G.; Hambsch, M.; Mannsfeld, S.; Voit, B.; Kiriy, A. Molecular Doping of a High Mobility Diketopyrrolopyrrole−Dithienylthieno [3, 2-B] Thiophene Donor−Acceptor Copolymer with F6TCNNQ. *Macromolecules* **2017**, *50*, 914−926.
(37) Fahlman, M.; Crispin, A.; Crispin, X.; Henze, S. K. M.; de Jong, M. P.; Osikowicz, W.; Tengstedt, C.; Salaneck, W. R. Electronic Structure of Hybrid Interfaces for Polymer-Based Electronics. *J. Phys.: Condens. Matter* **2007**, *19*, 183202.
(38) Nielsen, C. B.; Turbiez, M.; McCulloch, I. Recent Advances in the Development of Semiconducting Dpp-Containing Polymers for Transistor Applications. *Adv. Mater.* **2013**, *25*, 1859−1880.
(39) Li, Y.; Sonar, P.; Murphy, L.; Hong, W. High Mobility Diketopyrrolopyrrole (Dpp)-Based Organic Semiconductor Materials for Organic Thin Film Transistors and Photovoltaics. *Energy Environ. Sci.* **2013**, *6*, 1684−1710.
(40) Zhang, X.; Richter, L. J.; DeLongchamp, D. M.; Kline, R. J.; Hammond, M. R.; McCulloch, I.; Heeney, M.; Ashraf, R. S.; Smith, J. N.; Anthopoulos, T. D.; Schroeder, B.; Geerts, Y. H.; Fischer, D. A.; Toney, M. F. Molecular Packing of High-Mobility Diketo Pyrrolo-Pyrrole Polymer Semiconductors with Branched Alkyl Side Chains. *J. Am. Chem. Soc.* **2011**, *133*, 15073−15084.
(41) Liang, Z.; Zhang, Y.; Souri, M.; Luo, X.; Boehm, A. M.; Li, R.; Zhang, Y.; Wang, T.; Kim, D.-Y.; Mei, J.; Marder, S. R.; Graham, K. R. Influence of Dopant Size and Electron Affinity on the Electrical Conductivity and Thermoelectric Properties of a Series of Conjugated Polymers. *J. Mater. Chem. A* **2018**, *6*, 16495−16505.
(42) Jacobs, I. E.; Aasen, E. W.; Nowak, D.; Li, J.; Morrison, W.; Roehling, J. D.; Augustine, M. P.; Moulé, A. J. Direct-Write Optical Patterning of P3HT Films Beyond the Diffraction Limit. *Adv. Mater.* **2017**, *29*, 1603221.
(43) Salzmann, I.; Heimel, G.; Oehzelt, M.; Winkler, S.; Koch, N. Molecular Electrical Doping of Organic Semiconductors: Fundamental Mechanisms and Emerging Dopant Design Rules. *Acc. Chem. Res.* **2016**, *49*, 370−378.
(44) Ghani, F.; Opitz, A.; Pingel, P.; Heimel, G.; Salzmann, I.; Frisch, J.; Neher, D.; Tsami, A.; Scherf, U.; Koch, N. Charge Transfer in and Conductivity of Molecularly Doped Thiophene-Based Copolymers. *J. Polym. Sci., Part B: Polym. Phys.* **2015**, *53*, 58−63.
(45) Jacobs, I. E.; Cendra, C.; Harrelson, T. F.; Bedolla Valdez, Z. I.; Faller, R.; Salleo, A.; Moulé, A. J. Polymorphism Controls the Degree of Charge Transfer in a Molecularly Doped Semiconducting Polymer. *Mater. Horiz.* **2018**, *5*, 655−660.
(46) Tietze, M. L.; Pahner, P.; Schmidt, K.; Leo, K.; Lüssem, B. Doped Organic Semiconductors: Trap-Filling, Impurity Saturation, and Reserve Regimes. *Adv. Funct. Mater.* **2015**, *25*, 2701−2707.
(47) Li, J.; Zhao, Y.; Tan, H. S.; Guo, Y.; Di, C.-A.; Yu, G.; Liu, Y.; Lin, M.; Lim, S. H.; Zhou, Y.; Su, H.; Ong, B. S. A Stable Solution-Processed Polymer Semiconductor with Record High-Mobility for Printed Transistors. *Sci. Rep.* **2012**, *2*, 754.
(48) Ha, J. S.; Kim, K. H.; Choi, D. H. 2,5-Bis(2-octyldodecyl)-pyrrolo[3,4-C]pyrrole-1,4-(2H,5H)-dione-Based Donor−Acceptor Alternating Copolymer Bearing 5,5′-Di(thiophen-2-yl)-2,2′-biselenophene Exhibiting 1.5 $Cm^2 \cdot V^{-1} \cdot S^{-1}$ Hole Mobility in Thin-Film Transistors. *J. Am. Chem. Soc.* **2011**, *133*, 10364−10367.
(49) Di Pietro, R.; Erdmann, T.; Carpenter, J. H.; Wang, N.; Shivhare, R. R.; Formanek, P.; Heintze, C.; Voit, B.; Neher, D.; Ade, H.; Kiriy, A. Synthesis of High-Crystallinity Dpp Polymers with Balanced Electron and Hole Mobility. *Chem. Mater.* **2017**, *29*, 10220−10232.
(50) Noriega, R.; Rivnay, J.; Vandewal, K.; Koch, F. P. V.; Stingelin, N.; Smith, P.; Toney, M. F.; Salleo, A. A General Relationship between Disorder, Aggregation and Charge Transport in Conjugated Polymers. *Nat. Mater.* **2013**, *12*, 1038−1044.
(51) Li, J.; Holm, D. M.; Guda, S.; Bedolla-Valdez, Z. I.; Gonel, G.; Jacobs, I. E.; Dettmann, M. A.; Saska, J.; Mascal, M.; Moulé, A. J. Effect of Processing Conditions on Additive Disc Patterning of P3HT Films. *J. Mater. Chem. C* **2019**, *7*, 302−313.

DOI: 10.1021/acs.chemmater.8b04150
Chem. Mater. 2019, 31, 1500−1506